Living Clusters and Crystals from Low-Density Suspensions of Active Colloids

B. M. Mognetti,[1] A. Šarić,[1,2] S. Angioletti-Uberti,[1,3] A. Cacciuto,[2] C. Valeriani,[4,*] and D. Frenkel[1]

[1]*Deparment of Chemistry, University of Cambridge, Lensfield Road, Cambridge CB2 1EW, United Kingdom*
[2]*Department of Chemistry, Columbia University, 3000 Broadway, New York, New York 10027, USA*
[3]*Institute of Physics, Humboldt Universität zu Berlin, Newtonstraße 15, 12489 Berlin, Germany*
[4]*Departamento de Quimica Fisica I, Facultad de Ciencias Qumicas, Universidad Complutense de Madrid, 28040 Madrid, Spain*

(Received 1 July 2013; published 11 December 2013)

Recent studies aimed at investigating artificial analogs of bacterial colonies have shown that low-density suspensions of self-propelled particles confined in two dimensions can assemble into finite aggregates that merge and split, but have a typical size that remains constant (living clusters). In this Letter, we address the problem of the formation of living clusters and crystals of active particles in three dimensions. We study two systems: self-propelled particles interacting via a generic attractive potential and colloids that can move toward each other as a result of active agents (e.g., by molecular motors). In both cases, fluidlike "living" clusters form. We explain this general feature in terms of the balance between active forces and regression to thermodynamic equilibrium. This balance can be quantified in terms of a dimensionless number that allows us to collapse the observed clustering behavior onto a universal curve. We also discuss how active motion affects the kinetics of crystal formation.

DOI: 10.1103/PhysRevLett.111.245702 PACS numbers: 82.70.Dd, 05.65.+b, 64.75.Yz

Active systems consume energy that keeps them in an out-of-equilibrium state [1,2]. This is typical for many biologically relevant systems, which by exploiting chemical energy can self-organize into complex structures that lack any equilibrium counterpart. Examples are abundant and exist at different length scales: from cytoskeleton remodulation during cell mitosis [3] to swarming phenomena in microswimmers or flocks of birds [4,5]. The similarity of the patterns displayed by these systems leads many to address the general principles behind their formation using simple models [6]. The reproducibility and robustness of the phenomena under a variety of external conditions motivated the creation of a large body of research on the self-assembly of active particles as a possible strategy towards the fabrication of new functional nano- and mesoscopic structures [7]. In this respect, there have been several efforts to study active self-organization in a tightly controlled environment, with the most-studied systems being self-propelled particles [6,8–11] and active gels (e.g., Ref. [12]).

Recently, two experimental groups have shown how two-dimensional (2D) suspensions of self-propelled (SP) colloids (moving through the consumption of an appropriate "fuel") self-assemble into dynamic clusters that constantly join and split, recombining with each other to reach a steady state [13,14]. A general understanding of active cluster formation is lacking, but different explanations have been proposed. The authors of Ref. [13] argued that a net attraction between colloids is responsible for clustering. This attraction is due to nonuniformity in the chemical fuel concentration between two colloids. This was confirmed by Ref. [14], which also found a $1/d^2$ dependence of the particle-particle attraction (d being the interparticle distance). The formation of finite-size clusters has been also observed in low density bacteria/polymer suspensions, at intermediate polymer concentrations just before phase separation [10]. However, in other recent studies (e.g., Refs. [9,11,15,16]) clusters were shown to form due to dynamic instabilities; hence, attraction cannot be singled out as the only cause promoting aggregation in active systems.

Doubts remain over the nature of the driving forces behind the clustering observed in different experiments. Furthermore, it is not clear whether this phenomenon is specific to these systems or a generic feature of nonequilibrium.

To address these questions, in this Letter we report and explain the formation of living clusters in two very different active systems and at arbitrarily low packing fraction. The first system consists of SP particles similar to those used in Refs. [13,14] with an added isotropic attraction. The second system is of hard spheres that, when closer than a given range, are brought together by molecular motors acting as dynamical cross-links between "tracks" (e.g., microtubules) grafted to the particles. The model was inspired by recent work in which centrosomes [17] were self-assembled with the microtubule polarity constrained to point inward or outward [18]. Note that in this model, the motors' action leads to a net attraction between particles. We refer to these particles as self-displacing (SD). To highlight the difference between the models, consider that in the absence of activity and at the packing fractions used in this study (2 orders of magnitude below hard sphere freezing) SP particles would condense, whereas SD particles would remain in the gas phase. Furthermore, the role of activity in the two systems is inverted; in the SP model it

tends to break up clusters, whereas for SD particles it drives their formation, and the splitting is instead due to diffusion.

By comparing these two different systems, we show that the assembly of finite-sized clusters at low packing fraction is a generic feature of suspensions of active colloids and it is not limited to the systems studied in Refs. [13,14]. Moreover, we demonstrate that the formation of finite aggregates can be interpreted as a competition between equilibrium and active forces.

Simulation details.—Self-propelled colloids are modelled as spherical particles of diameter $\sigma_p = 10\sigma$ (where σ is the MD unit of length) interacting via a Lennard-Jones potential

$$V(r_{ij}) = 4\epsilon\left[\left(\frac{\sigma_p}{r_{ij}}\right)^{12} - \left(\frac{\sigma_p}{r_{ij}}\right)^{6}\right], \quad (1)$$

truncated and shifted at $2.5\sigma_p$. Self-propulsion is implemented by adding a constant force $\boldsymbol{F}$ acting along a predefined axis through the colloid [see Fig. 1(a)]. To enable the rotation of the axis of the colloid, and therefore the direction of its propulsion, two small ideal particles with diameter σ are placed inside each colloid along its axis and positioned 4.5σ symmetrically with respect to the center of the particle, forming a rigid body with the colloid. Though the small particles do not interact with any other particle in the system, they are however subjected to the thermal fluctuations induced by the bath, thus leading to a net Brownian rotation of their axis. The motion of each particle (colloids and ideal particles) is governed by the Langevin equation:

$$m\ddot{\boldsymbol{r}}_{\boldsymbol{i}} = -\sum_{j\neq i}\frac{\partial V(r_{ij})}{\partial \boldsymbol{r}_{\boldsymbol{i}}} - \zeta\dot{\boldsymbol{r}}_{\boldsymbol{i}} + \boldsymbol{F}_{\boldsymbol{i}} + \boldsymbol{F}_{\boldsymbol{R,i}} \quad (2)$$

where m is the particle's mass, set to 1, and ζ is the friction coefficient ($\zeta = m\gamma$ with damping coefficient γ). $F_{R,i} = \sqrt{k_B T\zeta}R_i(t)$ is the random force due to the solvent, where $R_i(t)$ is a stationary Gaussian noise with zero mean and variance $\langle R_i(t)R_j(t')\rangle = \delta(t-t')\delta_{ij}$. The damping parameter is $\gamma = \tau^{-1}$, τ being the MD unit of time. Simulations were performed at two different packing fractions $\phi = 0.01$ and $\phi = 0.1$, using the code LAMMPS [19] with a total number of particles of $N_{\text{part}} = 1728$ for at least 15×10^6 time steps (being $\Delta t = 0.008\tau$). Each simulation was repeated between 4 and 16 times with different initial random velocities.

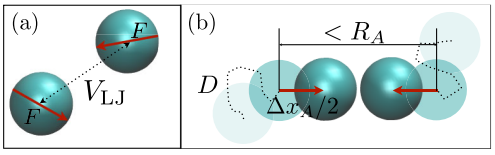

FIG. 1 (color online). (a) SP particles (with propulsion force F) interacting via a Lennard-Jones potential. (b) SD particles moving towards each other over a distance Δx_A with a rate ν if they are within a distance R_A. Particles also undergo diffusion (D). Depending on the values of Δx_A, ν, and D, either clustering or collisions dominate.

SD colloids are modeled as hard spheres with diameter σ following Brownian motion with diffusion constant D. Whenever two (randomly chosen) particles are closer than a given distance (R_A), they can be self-displaced toward each other along the direction joining their centers. The activity of SD colloids is then specified by the range R_A within which particles can be cross-linked, the rate ν at which pulling events occur, and Δx_A, the size of the active displacement [see Fig. 1(b)]. In this work, we set $R_A = 2\sigma$. The dynamics is implemented using a Monte Carlo algorithm generating diffusive or attractive displacements with the correct frequencies. For a given "pulling" rate ν, we randomly select a colloid i and one of its neighbors j. Particles i and j are then moved toward each other over a distance $\min[\Delta x_A, r_{ij} - \sigma]$, unless this motion results in an overlap with a third colloid. The active displacement does not alter the center of mass (c.m.) of the two colloids. If $\Delta x_A \geq R_A - \sigma$, the colloids are displaced to their closest possible configuration. We call this the "processive limit" because molecular motors will drag the two colloids until the end of the microtubule is reached. Simulations with SD colloids were performed with $N_{\text{part}} = 1000$ and $N_{\text{part}} = 2000$.

Aggregation of living clusters.—One of the most interesting results of our simulations is that, despite being fundamentally different, both models lead to the formation of disordered "living" aggregates. The degree of clustering is measured using the function

$$\Theta = 1 - \frac{1}{\langle S_{\text{clust}}\rangle}, \quad (3)$$

where $\langle S_{\text{clust}}\rangle$ is the average number of particles in a cluster; Θ ranges from 0 in the gas phase ($\langle S_{\text{clust}}\rangle = 1$) to $1 - 1/N_{\text{part}} \approx 1$ when all atoms belong to a single cluster ($\langle S_{\text{clust}}\rangle = N_{\text{part}}$). Two particles are defined as clustered whenever $r_{ij} < 1.2\sigma_p$ (for SP particles) or if $r_{ij} < R_A$ (for SD particles). The number and morphology of the clusters depend on the relative ratio between equilibrium and out-of-equilibrium control parameters, as measured by a dimensionless quantity that we call the propensity for aggregation P_{agg}. In the case of SP colloids, P_{agg} is simply the ratio between the strength of the attraction between particles and the propelling force $P_{\text{agg,SP}} \equiv \epsilon/(F\sigma_p)$, whereas for SD colloids, P_{agg} is the ratio between the times to move colloids actively and diffusively over a distance of $R_A - \sigma$, $P_{\text{agg,SD}} = \nu/[2D/(R_A - \sigma)^2]$.

Figure 2(a) shows the number of clusters per particles in the SP colloidal suspension for different values of ϵ and F. These data represent the steady-state value for the cluster distribution, to which different initial states converge after a short transient time. Strikingly, all data collapse onto a single master curve when plotted as a function of $P_{\text{agg,SP}}$.

Furthermore, the figure shows a linear increase in the degree of clustering with decreasing activity (i.e., increasing $P_{\mathrm{agg,SP}}$), which supports the simple picture of the mechanism of cluster formation in terms of two competing terms: the LJ attraction drives aggregation, whereas activity counteracts the formation of large clusters.

Figure 2(b) shows the same analysis for SD colloids in the processive limit ($\Delta x_A > R_A - \sigma$) at a colloidal packing fraction of 8×10^{-3}. In this case, clustering is observed when activity increases. The trend is opposite to that observed in Fig. 2(a) for SP particles because, as discussed above, in the SD suspension activity is responsible for aggregation, whereas for SP particles activity is the limiting factor for cluster formation. Increasing the colloidal diffusivity increases the probability of a colloid to detach from the cluster. Interestingly, as in the SP system, the number of clusters exhibits a linear dependence on $P_{\mathrm{agg,SD}}$. However, as we approach the limit in which a single big cluster forms (see Fig. 2), we observe that the relaxation time required to reach the steady state increases sensibly, suggesting the presence of a phase transition. We defer this issue to a future study.

In both systems, we find that the cluster size distribution appears to follow a power law [see insets in Fig. 2(a)]. Clusters coexist with a monomer-rich gas phase. The clusters grow and shrink dynamically. An analysis of the pair correlation function [inset of Fig. 2(b)] does not reveal any sign of structural order at longer range than the typical cluster size. It is important to mention that we see living clusters for very different initial conditions. Specifically, the same living clusters configurations were observed when we started simulations from a dense state (perfect crystal). Notice that living clusters form in the region where $P_{\mathrm{agg,SP}} \approx 0.1$–$0.5$ and $P_{\mathrm{agg,SD}} \approx 1$–$5$, i.e., where active and thermal forces have comparable magnitude. This highlights the synergic nature of these nonequilibrium aggregates. Similar power-law behavior for cluster size distributions has also been observed as a function of energy intake and particle density in a recent study on active Brownian particles [20].

Interestingly, when SP particles were confined to move in 2D, for moderate $P_{\mathrm{agg,SP}}$ we obtained living clusters with crystalline order analogous to those observed in the experiments of Ref. [14]. However, we never observed living clusters with crystalline order in 3D in the regime where active and thermal forces have comparable magnitude.

Driven phase diagram of the SD suspension.—In the SD suspension, activity is controlled not only by the pulling rate but also by the size of the active displacement Δx_A. In Fig. 3(a), we show how clustering is altered by the latter parameter. As expected, in decreasing Δx_A the degree of clustering can be kept constant by increasing ν.

In Fig. 3(b), we investigate the change in the number of clusters as a function of the number density ρ. More

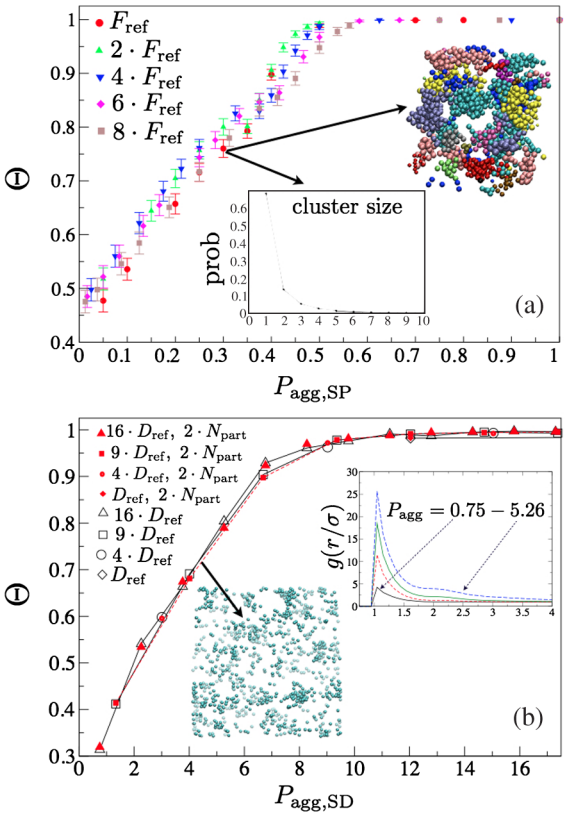

FIG. 2 (color online). Degree of clustering Θ versus aggregation propensity (see text for the definitions) for the SP (a) and the SD systems (b). Results for several propulsion forces F (a) and diffusion coefficients D (b) collapse onto two universal curves. The insets represent typical snapshots of living clusters, the cluster size distribution function (a), and the pair distribution function (b) at significant P_{agg} where finite clusters form. Particles belonging to different clusters in (a) are colored differently and, for clarity, monomers and small clusters are not shown. In the SP case, $\phi = 0.1$ and $F_{\mathrm{ref}}\sigma_p = 10k_BT$, whereas in the SD case $d_{\mathrm{c.m.}}/R_A = 2$ ($\phi = 0.008$), $N_{\mathrm{part}} = 1000$, and $D_{\mathrm{ref}} = 0.01\sigma/\tau_{MC}$, τ_{MC} being the simulation time unit.

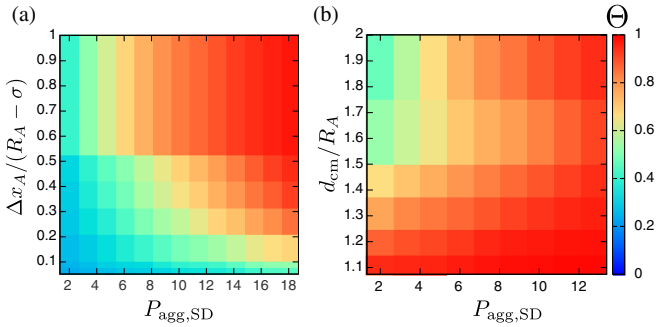

FIG. 3 (color online). (a) Fraction of clusters in the SD suspension as a function of the processivity parameter $\Delta x_A/(R_A - \sigma)$ versus the aggregation propensity $P_{\mathrm{agg,SD}}$ and (b) as a function of their average distance $d_{\mathrm{c.m.}} = \rho^{-1/3}$ versus $P_{\mathrm{agg,SD}}$. In (a), $d_{\mathrm{c.m.}}/R_A = 2$ ($\phi = 0.008$).

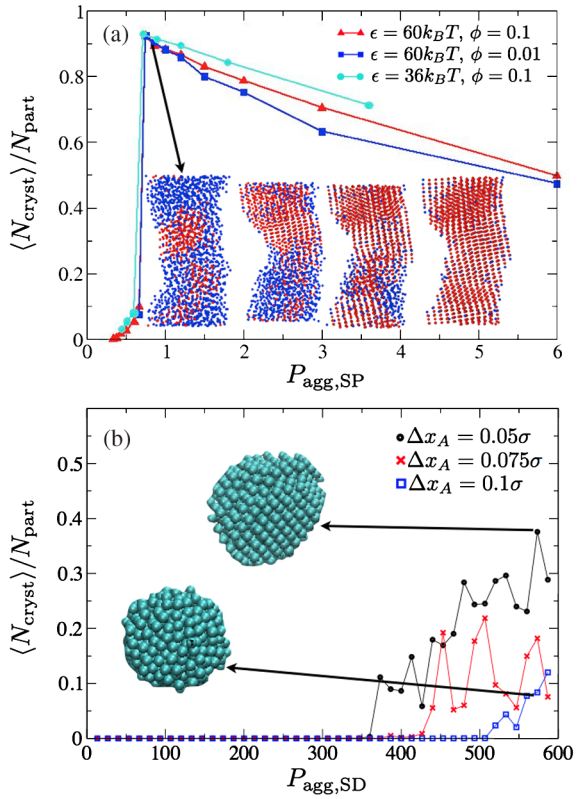

FIG. 4 (color online). Crystallization of active particles. Fraction of solidlike particles in the system versus the aggregation propensity in the SP (a) and SD (b) cases. The snapshots in (a) show the crystallization process of a single cluster ($\phi = 0.1$, $\epsilon = 60k_BT$, and $F\sigma_p = 80k_BT$) during the course of a simulation. Fluidlike particles are depicted in blue, with solidlike particles in red. Crystals span the whole simulation box. (b) SD particles at low $\Delta x_A/\sigma$ form small faceted crystals that are replaced by arrested aggregates when Δx_A increases (inset snapshots). In this case, $d_{\rm c.m.}/R_A = 2$ ($\phi = 0.008$).

specifically, we plot it as a function of the average distance between colloids in the bulk, $d_{\rm c.m.} = \rho^{-1/3}$. Not surprisingly, a larger degree of activity is required to maintain clustering at large values of $d_{\rm c.m.}$. Both Figs. 2 and 3 suggest the presence of a dynamical transition in which the number of clusters varies continuously from 1 to a finite fraction.

Active crystallization.—Beyond a well-defined onset value of $P_{\rm agg}$, we observe cluster crystallization. Crystallinity of the aggregates is detected by evaluating the q_6 bond-order parameter and using the criteria described in Refs. [21,22]. Figure 4 shows the fraction of solidlike particles as a function of $P_{\rm agg,SP}$ for suspensions of SP (a) and SD (b) particles. For SP particles [Fig. 4(a)], the fraction of crystalline particles exhibits a nonmonotonic behavior. For $\epsilon > F\sigma_p$ (in our simulations, $\epsilon \geq 30k_BT$ and $F\sigma_p \approx 10k_BT$), we observe the formation of disordered structures that survive throughout the simulation. Formation of the equilibrium crystalline phase at high values of ϵ is kinetically hindered by the strong interparticle attraction, which leads to low diffusivity and, hence, long equilibration times. In the opposite regime, when $\epsilon \approx 0.1F\sigma_p$ (i.e., $P_{\rm agg,SP} \approx 0.1$), the living fluid aggregates described in Fig. 2 make their appearance. At intermediate values of $\epsilon/F\sigma_p$ [see Fig. 4(a)] instead, the balance between particle attraction and activity leads to the formation of crystalline clusters. A possible interpretation of these results is that in this intermediate regime, the role of activity is that of speeding, up the kinetics of crystal formation by increasing the diffusivity, allowing a faster annealing of defects.

It is instructive to relate the simulation parameters in the SP case to the experimental systems discussed in Refs. [13–16]. If a colloid of $\sigma_p = 1$ μm is propelling with $v \sim 5$ μm/s, its propulsion force in water is $F \sim 0.05$ pN. Our analysis suggests that the interaction strength between the colloids required to form a single macroscopic fluid cluster should be $\epsilon \sim 6k_BT$ ($P_{\rm agg,SP} \approx 0.5$). For lower attractions, the system forms many living clusters, as typically observed in experiments. According to Fig. 4(a), a well-ordered crystal of active particles should be expected within a few seconds for $\epsilon \sim 12k_BT$.

Figure 4(b) shows the crystallization route followed by SD particles. In this system, crystals only form for small displacements. When the processivity parameter $\Delta x_A > 0.1$, aggregates instead undergo structural arrest before they can rearrange into an ordered structure. We believe that the formation of regular structures with SD particles is similar to crystallization in an external field (e.g., Refs. [23,24]). However, here, the effective external forces push the particles toward the center of a cluster. It should be stressed that in both our systems crystallization typically leads to irreversible clustering rather than to an equilibrium size distribution of living clusters.

Conclusion.—In this Letter, we investigated the formation of living fluidlike clusters and crystals from low-density suspensions of active colloids. We studied two different systems: self-propelled particles interacting via an attractive potential and hard spheres in which colloids are pairwise self-displaced toward each other. In both cases, we observed the formation of living fluid clusters (as in Refs. [13,14]) and irreversible crystals of active particles. We showed how the formation of finite aggregates can be ascribed to a balanced competition between equilibrium forces and activity, regardless of the nature of the latter. Furthermore, we demonstrated that activity aids annealing defects in crystalline clusters.

B. M. M. and A. S. contributed equally to this work. This work was supported by the ERC Advanced Grant 227758, the National Science Foundation under Career Grant No. DMR-0846426, the Wolfson Merit Award 2007/R3 of the Royal Society of London, and the EPSRC Programme Grant EP/I001352/1. B. M.M . acknowledges T. Curk and A. Ballard for useful discussions. C. V. acknowledges financial support from a Juan de la Cierva Fellowship, from the

Marie Curie Integration Grant PCIG-GA-2011-303941 ANISOKINEQ, and from the National Project FIS2010-16159. S. A.-U. acknowledges support from the Alexander von Humboldt Foundation.

*Corresponding author.
cvaleriani@quim.ucm.es

[1] B. Schmittmann and R. K. P. Zia, *Statistical Mechanics of Driven Diffusive Systems*, in Phase Transitions and Critical Phenomena, edited by C. Domb and J. L. Lebowitz (Academic, New York, 1995), Vol. 17, p. 1.
[2] M. C. Marchetti, J.-F. Joanny, S. Ramaswamy, T. B. Liverpool, J. Prost, M. Rao, and R. S. Simha, Rev. Mod. Phys. **85**, 1143 (2013).
[3] B. Alberts, A. Johnson, J. Lewis, M. Raff, K. Roberts, and P. Walter, *Molecular Biology of the Cell* (Garland Science, New York, 2002), 4th ed.
[4] Y. Katz, C. C. Ioannou, K. Tunstro, C. Huepe, and I. D. Couzin, Proc. Natl. Acad. Sci. U.S.A. **108**, 18 720 (2011); A. Cavagna, A. Cimarelli, I. Giardina, G. Parisi, R. Santagati, F. Stefanini, and M. Viale, Proc. Natl. Acad. Sci. U.S.A. **107**, 11 865 (2010).
[5] M. Rubenstein, C. Ahler, and R. Nagpal, *IEEE International Conference on Robotics and Automation (IRCA), St. Paul, MN, May 14–18, 2012* (IEEE, New York, 2002).
[6] T. Vicsek, A. Czirók, E. Ben-Jacob, I. Cohen, and O. Shochet, Phys. Rev. Lett. **75**, 1226 (1995).
[7] R. Galland, P. Leduc, C. Gurin, D. Peyrade, L. Blanchoin, and M. Thry, Nat. Mater. **12**, 416 (2013).
[8] A. Baskaran and M. C. Marchetti, Phys. Rev. Lett. **101**, 268101 (2008).
[9] J. Stenhammar, A. Tiribocchi, R. J. Allen, D. marenduzzo, and M. Cates, Phys. Rev. Lett. **111**, 145702 (2013).
[10] J. Schwarz-Linek, C. Valeriani, A. Cacciuto, M. E. Cates, D. Marenduzzo, A. N. Morozov, and W. C. K. Poon, Proc. Natl. Acad. Sci. U.S.A. **109**, 4052 (2012).
[11] G. S. Redner, A. Baskaran, and M. F. Hagan, Phys. Rev. E **88**, 012305 (2013).
[12] S. Wang and P. G. Wolynes, Proc. Natl. Acad. Sci. U.S.A. **108**, 15184 (2011).
[13] I. Theurkauff, C. Cottin-Bizonne, J. Palacci, C. Ybert, and L. Bocquet, Phys. Rev. Lett. **108**, 268303 (2012).
[14] J. Palacci, S. Sacanna, A. P. Steinberg, D. J. Pine, and P. M. Chaikin, Science **339**, 936 (2013).
[15] I. Buttinoni, J. Bialke, F. Kümmel, H. Löwen, C. Bechinger, and T. Speck, Phys. Rev. Lett. **110**, 238301 (2013).
[16] Y. Fily and M. C. Marchetti, Phys. Rev. Lett. **108**, 235702 (2012).
[17] E. D. Spoerke, G. D. Bachand, J. Liu, D. Sasaki, and B. C. Bunker, Langmuir **24**, 7039 (2008).
[18] Molecular motors are not present in the system of Ref. [17]. Here, we use the concept of synthetic centrosomes as a possible realization of SD particles.
[19] S. J. Plimpton, J. Comput. Phys. **117**, 1 (1995).
[20] V. Lobaskin and M. Romenskyy, Phys. Rev. E **87**, 052135 (2013).
[21] S. Auer and D. Frenkel, Annu. Rev. Phys. Chem. **55**, 333 (2004).
[22] Two particles i and j are considered bonded if their center of the mass distance is $r_{ij} < 1.25 \times \sigma_p$ (in the case of SP particles) or if $r_{ij} < R_A$ (for SD particles). Therefore, a particle is identified as solidlike if it is bonded to more than 7 neighbors and if $q_6(i) \times q_6(j) > 0.5$.
[23] R. Piazza, T. Bellini, and V. Degiorgio, Phys. Rev. Lett. **71**, 4267 (1993); R. P. A. Dullens, D. G. A. L. Aarts, and W. K. Kegel, Phys. Rev. Lett. **97**, 228301 (2006).
[24] E. Allahyarov and H. Löwen, Europhys. Lett. **95**, 38 004 (2011).